Acta Cryst E CRYSTALLOGRAPHIC COMMUNICATIONS

ISSN 2056-9890

Synthesis, crystallographic analysis and Hirshfeld surface analysis of 4-bromo-2-{[2-(5-bromo-2-nitrophenyl)hydrazin-1-ylidene]methyl}-5-fluorophenol

Mavise Yaman,[a] Ercan Aydemir,[b,c] Necmi Dege,[a] Erbil Agar[b] and Turganbay S. Iskenderov[d]*

[a]Ondokuz Mayıs University, Faculty of Arts and Sciences, Department of Physics, 55139, Kurupelit, Samsun, Turkey, [b]Ondokuz Mayıs University, Faculty of Arts and Sciences, Department of Chemistry, 55139, Samsun, Turkey, [c]Ministry of Forestry and Water Affairs , 11th Regional Directorate, 55030, Ilkadım-Samsun, Turkey, and [d]Taras Shevchenko National University of Kyiv, Department of Chemistry, 64, Vladimirska Str., Kiev 01601, Ukraine. *Correspondence e-mail: tiskenderov@ukr.net

Received 10 October 2018
Accepted 16 October 2018

Edited by D.-J. Xu, Zhejiang University (Yuquan Campus), China

Keywords: crystal structure; Hirshfeld surface; Hydrazone; crystal structure; hydrogen bonding; 5-bromo-4-fluoro-2-hydroxybenzaldehyde.

CCDC reference: 1864935

Supporting information: this article has supporting information at journals.iucr.org/e

The title compound, $C_{13}H_8Br_2FN_3O_3$, is nearly planar with a dihedral angle of 10.6 (4)° between the two benzene rings. Intramolecular N—H···O and O—H···N hydrogen bonds occur. In the crystal, the molecules are linked by weak C—H···O and C—H···Br hydrogen bonds. The roles of the intermolecular interactions in the crystal packing were clarified using Hirshfeld surface analysis.

1. Chemical context

Hydrazones, the most important derivatives of carboxaldehyde, are widely used both in organic synthesis and in industrial work because of their reaction abilities, such as ring closing, oxidation-reduction, replacement reactions and coupling (Öztürk *et al.*, 2003). They are generally considered to be useful starting materials for the production of pharmaceuticals, pesticides, textile dyestuffs as well as compounds that serve as stabilizers and inhibitors in photography (Kaban & Ocal, 1993). In addition, they exhibit a wide range of applications in the fields of biology, optics, catalysis and analytical chemistry. Their broad spectrum of biological activities includes antimicrobial, antifungal, antiviral, antitumor, anti-HIV, anti-inflammatory, antineoplastic and analgesic activities (Sudheer *et al.*, 2015; Soujanya & Rajitha, 2017). Hydrazone-based molecular switches, metalloassemblies and sensors have also been developed (Sudheer *et al.*, 2015). Unlike oximes (Sliva *et al.*, 1997; Penkova *et al.*, 2010; Pavlishchuk *et al.*, 2010), hydrazones are mostly obtained as a mixture of *E* and *Z* isomers and both isomers are generally weak acids (Mori *et al.*, 2015). Tautomerism between the isomers might also occur in the case of the hydrazone and azo forms (Aydemir & Kaban, 2018). In this study, the structure of the newly synthesized compound has been evaluated by spectroscopic techniques. In view of this, in order to obtain information about the stereochemistry of the molecule and to confirm the assigned structure, X-ray analysis of the title compound was undertaken.

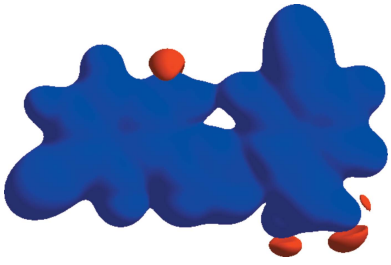

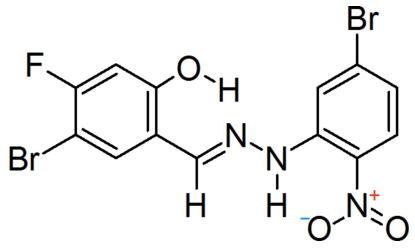

2. Structural commentary

The molecular structure of the title compound is illustrated in Fig. 1. The dihedral angle between the aromatic rings is 10.6 (4)°. The N1—N2 and N2–C8 bond lengths are 1.368 (7) and 1.374 (8) Å, respectively. The C13–N3 bond [1.451 (8) Å] in the nitro group is close to the standard value for this type of bond (Allen *et al.*, 1987). Intramolecular N2—H2···O3 and O1—H1···N1 hydrogen-bonding interactions (Table 1) occur.

3. Supramolecular features

In the crystal, the molecules are linked by weak C—H···O and C—H···Br hydrogen bonds (Table 1, Fig. 2).

4. Hirshfeld surface analysis

A Hirshfeld surface analysis was performed to quantify the nature of the intermolecular interactions. The Hirshfeld surfaces were generated using *CrystalExplorer17.5* (Turner *et al.*, 2017) using a standard (high) surface resolution. Fig. 3 shows the Hirshfeld surfaces mapped over d_{norm} in the range −0.2247 (red) to 1.3787 (blue) a.u. If the value of d_{norm} is negative, the intermolecular contacts are shorter than the van der Waals radius; these are shown as red regions. A positive value of d_{norm}, shown in blue, indicates that the intermolecular contacts are longer than the van der Waals radius (Şen *et al.*, 2017). The red regions on the d_{norm} surface correspond to C—H···O hydrogen-bonding interactions, which comprise 20.2% of the total Hirshfeld surfaces.

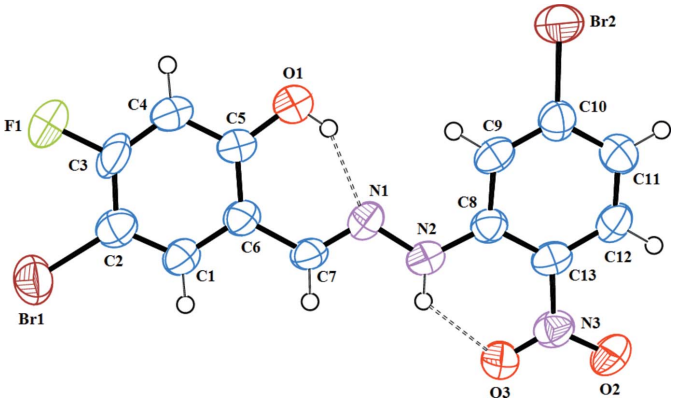

Figure 1
An *ORTEP* view of 4-bromo-2-{[2-(5-bromo-2-nitrophenyl)hydrazin-1-ylidene]methyl}-5-fluorophenol. Displacement ellipsoids are drawn at the 50% probability level.

Table 1
Hydrogen-bond geometry (Å, °).

D—H···*A*	*D*—H	H···*A*	*D*···*A*	*D*—H···*A*
O1—H1···N1	0.82	1.91	2.631 (7)	146
N2—H2···O3	0.86	2.01	2.619 (7)	127
N2—H2···O3^{i}	0.86	2.50	3.293 (7)	155
C4—H4···O1^{ii}	0.93	2.60	3.494 (8)	162
C7—H7···O3^{i}	0.93	2.66	3.461 (7)	145
C12—H12···Br1^{iii}	0.93	3.02	3.908 (7)	161

Symmetry codes: (i) $-x+1, -y+1, -z+1$; (ii) $-x, -y+1, -z+1$; (iii) $x+\frac{1}{2}, -y+\frac{1}{2}, z+\frac{1}{2}$.

The two-dimensional fingerprint (FP) plots are used to analyse significant differences between the intermolecular interaction patterns (Gumus *et al.*, 2018; Kansız & Dege, 2018; Kansiz *et al.*, 2018). Fig. 4 represents the FP plot for the sum of the contacts contributing to the Hirshfeld surface displayed in normal mode. In Fig. 5 distinct spikes indicate different interactions between two adjacent molecules in the crystal structure. The contribution from the Br···H/H···Br contacts make the largest (21.7%) to the Hirshfeld surface (Fig. 5*b*). The 20.2% contribution from the O—H···O hydrogen bond is seen as a pair of sharp spikes at $d_e + d_i = 2.3$ Å) in Fig. 5*a*. The distribution of positive and negative potential over the Hirshfeld surface is represented in Fig. 6 (positive electrostatic potential shown in blue region and negative electrostatic potential in red).

5. Database survey

There are no direct precedents for the structure of $C_{13}H_8Br_2FN_3O_3$ in the crystallographic literature (CSD,

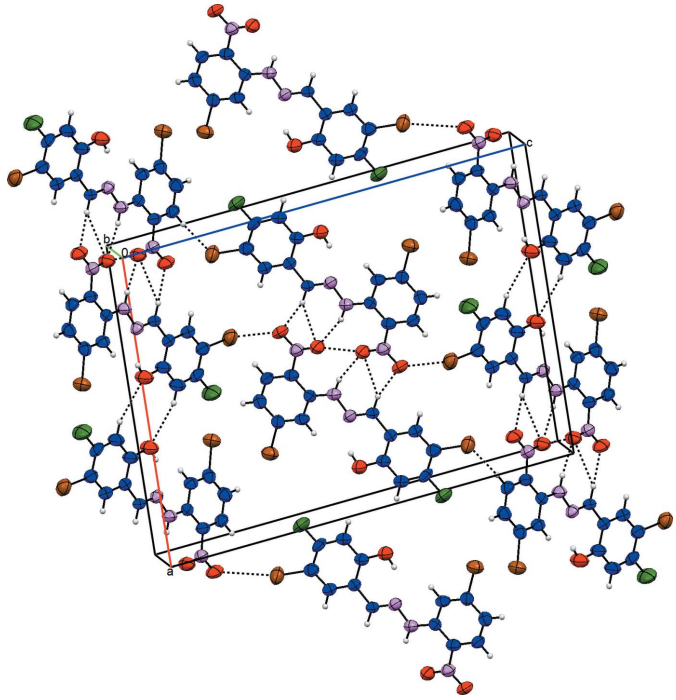

Figure 2
The view of the crystal packing of the title compound.

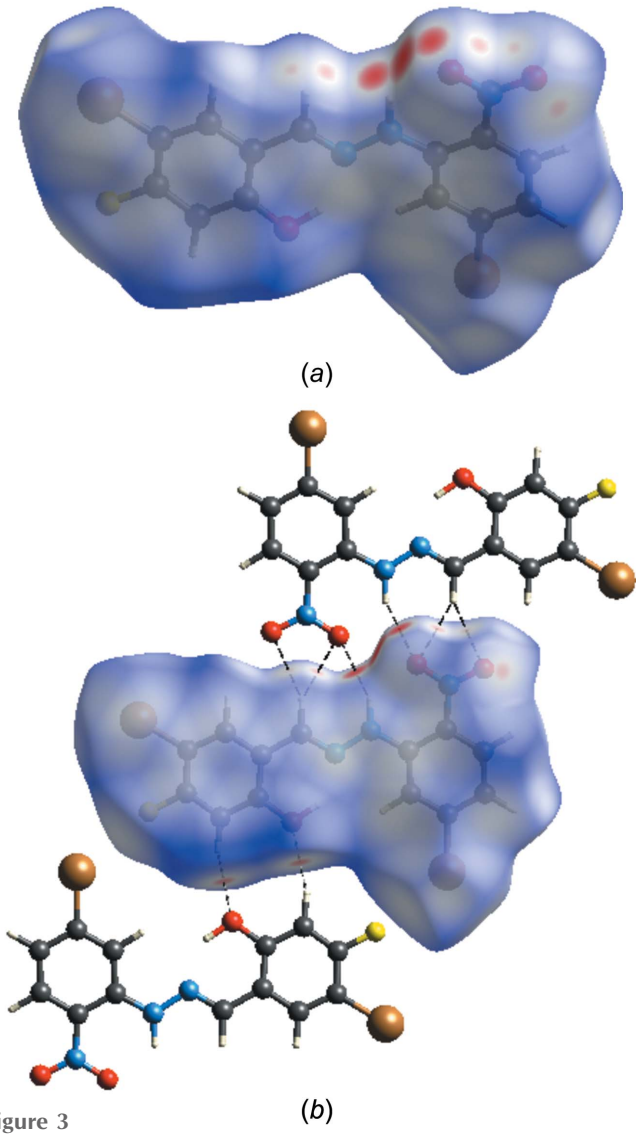

Figure 3
Views of the Hirshfeld surface of the title compound mapped over d_{norm}.

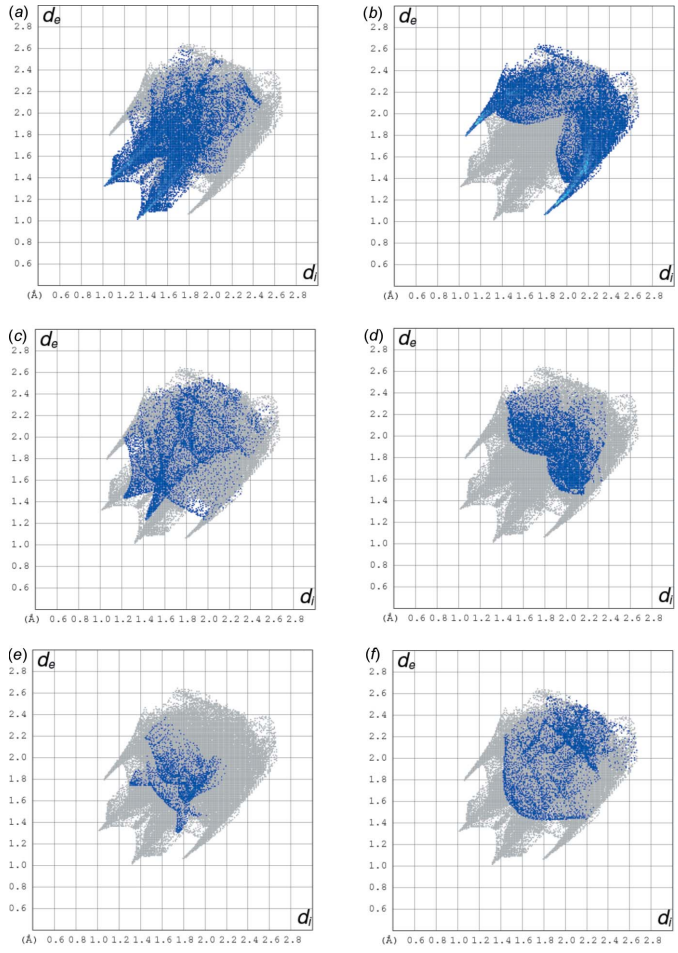

Figure 5
Two-dimensional fingerprint plots with a d_{norm} view of the (*a*) O···H/H···O (20.2%), (*b*) Br···H/H···Br (21.7%), (*c*) F···H/H···F (7.4%), (*d*) C···H/H···C (9.7%), (*e*) N···H/H···N (3.3%) and (*f*) H···H (6.0%) contacts in the title compound.

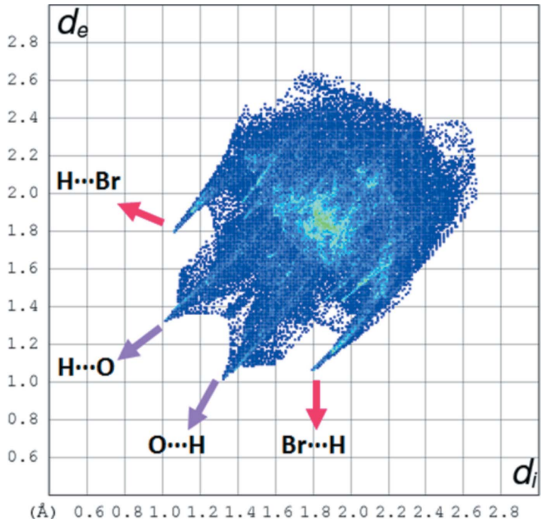

Figure 4
Fingerprint plot of the title compound showing all interactions.

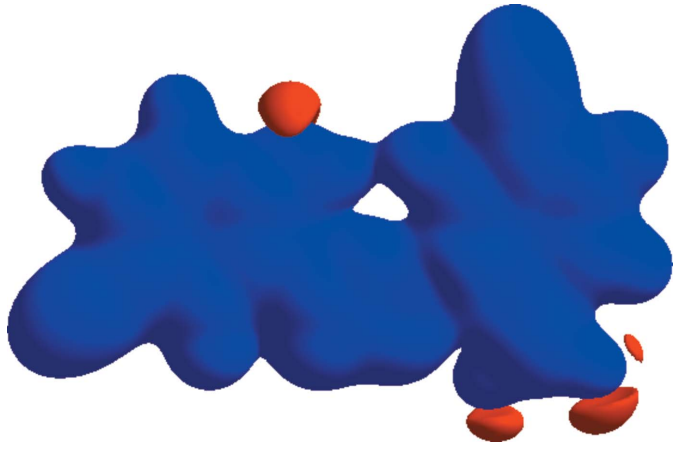

Figure 6
A view of the three-dimensional Hirshfeld surface of the title compound plotted over electrostatic potential.

version 5.39, update of May 2018; Groom *et al.*, 2016) but some similar structures including 2-nitrophenylhydrazine have been reported. All geometric parameters in the title compound agree well with those reported in the literature with the N1—N2 and N2—C8 bond distances being comparable to those in *N*-(4-chloro-2-nitrophenyl)-*N*′-methyl-*N*-(quinolin-4-ylmethylene)hydrazine [1.367 (2) and 1.386 (3) Å; Karadayı *et al.*, 2005] and *N*-(4-bromo-2-nitrophenyl)-*N*-methyl-*N*′-(quinolin-4-ylmethylene)hydrazine [1.359 (3) and 1.393 (4) Å; Öztürk *et al.*, 2003].

6. Synthesis and crystallization

5-Bromo-4-fluoro-2-hydroxybenzaldehyde (0.5 mmol) was dissolved in hot absolute ethanol (10 mL) and an equimolar amount of 5-bromo-2-nitrophenylhydrazine, dissolved in a minimum volume of absolute ethanol, was slowly added. The product appeared in the first minute. The reaction mixture was refluxed for an additional hour to complete the condensation and then allowed to cool in room temperature. The separated solid was then filtered and washed with ethanol and diethyl ether. The crude product was recrystallized from toluene as pink needle-shaped crystals, 96% yield, m.p. 569–570 K (dec.). The reaction scheme is shown in Fig. 7. UV ($CHCl_3$): λ_{max} 340, 430 nm; IR (KBr): υ 3610 (–OH), 3285 and 1155 (N—H), 3120–2985 (=C—H), 2915 (C—H), 1608 (C=N), 1558 (C=C), 1515 (N—N), 1475 and 1310 (N=O), 1195, 690 and 665 (C—*X*) cm^{-1}; MS (ESI^+): 434.01 ($[M + H]^+$, $C_{13}H_8Br_2FN_3O_3$; calculated 433.03).

7. Refinement

Crystal data, data collection and structure refinement details are summarized in Table 2. The C-bound hydrogen atoms were positioned geometrically and refined using a riding model: C—H = 0.93–0.97 Å with $U_{iso}(H) = 1.2U_{eq}(C)$

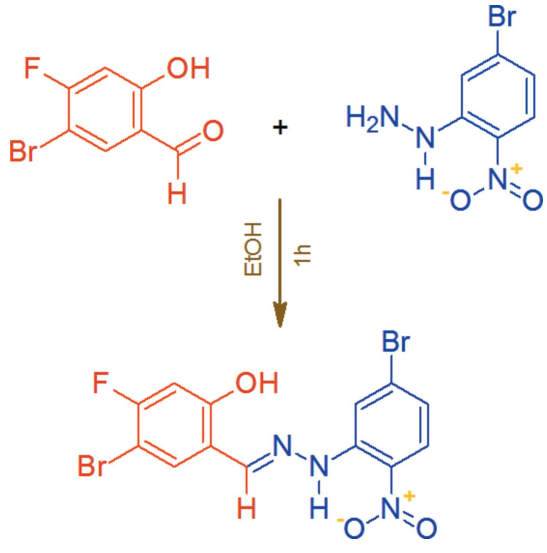

Figure 7
The synthesis of the title compound.

Table 2
Experimental details.

Crystal data	
Chemical formula	$C_{13}H_8Br_2FN_3O_3$
M_r	433.04
Crystal system, space group	Monoclinic, $P2_1/n$
Temperature (K)	296
a, *b*, *c* (Å)	16.1360 (14), 4.1745 (3), 21.468 (2)
β (°)	95.026 (7)
V (Å^3)	1440.5 (2)
Z	4
Radiation type	Mo $K\alpha$
μ (mm^{-1})	5.65
Crystal size (mm)	0.46 × 0.17 × 0.02
Data collection	
Diffractometer	Stoe IPDS 2
Absorption correction	Integration (*X-RED32*; Stoe & Cie, 2002)
T_{min}, T_{max}	0.296, 0.883
No. of measured, independent and observed [$I > 2\sigma(I)$] reflections	9546, 2775, 1270
R_{int}	0.113
$(\sin\theta/\lambda)_{max}$ (Å^{-1})	0.617
Refinement	
$R[F^2 > 2\sigma(F^2)]$, $wR(F^2)$, *S*	0.051, 0.098, 0.84
No. of reflections	2775
No. of parameters	200
H-atom treatment	H-atom parameters constrained
$\Delta\rho_{max}$, $\Delta\rho_{min}$ (e Å^{-3})	0.42, −0.28

Computer programs: *X-AREA* and *X-RED* (Stoe & Cie, 2002), *SHELXT2014* (Sheldrick, 2015*a*), *SHELXL2017* (Sheldrick, 2015*b*), *ORTEP-3 for Windows* and *WinGX* (Farrugia, 2012) and *PLATON* (Spek, 2009).

Acknowledgements

The authors acknowledge the Faculty of Arts and Sciences, Ondokuz Mayıs University, Turkey, for the use of the Stoe IPDS 2 diffractometer (purchased under grant F.279 of the University Research Fund).

References

Allen, F. H., Kennard, O., Watson, D. G., Brammer, L., Orpen, A. G. & Taylor, R. (1987). *J. Chem. Soc. Perkin Trans. 2*, pp. S1–S19.
Aydemir, E. & Kaban, S. (2018). *Asian J. Chem.* **30**, 1460–1464.
Farrugia, L. J. (2012). *J. Appl. Cryst.* **45**, 849–854.
Groom, C. R., Bruno, I. J., Lightfoot, M. P. & Ward, S. C. (2016). *Acta Cryst.* B**72**, 171–179.
Gumus, M. K., Kansiz, S., Dege, N. & Kalibabchuk, V. A. (2018). *Acta Cryst.* E**74**, 1211–1214.
Kaban, S. & Ocal, N. (1993). *Pak. J. Sci. Ind. Res.* **36**, 357–359.
Kansız, S. & Dege, N. (2018). *J. Mol. Struct.* **1173**, 42–51.
Kansiz, S., Macit, M., Dege, N. & Tsapyuk, G. G. (2018). *Acta Cryst.* E**74**, 1513–1516.
Karadayı, N., Aydemir, E., Kazak, C., Kirpi, E., Tuğcu, F. T., Gümüş, M. K. & Kaban, Ş. (2005). *Acta Cryst.* E**61**, o2671–o2673.
Mori, A., Suzuki, T. & Nakajima, K. (2015). *Acta Cryst.* E**71**, 142–145.
Öztürk, S., Akkurt, M., Aydemír, E. & Fun, H.-K. (2003). *Acta Cryst.* E**59**, o488–o489.
Pavlishchuk, A. V., Kolotilov, S. V., Zeller, M., Thompson, L. K., Fritsky, I. O., Addison, A. W. & Hunter, A. D. (2010). *Eur. J. Inorg. Chem.* pp. 4851–4858.
Penkova, L., Demeshko, S., Pavlenko, V. A., Dechert, S., Meyer, F. & Fritsky, I. O. (2010). *Inorg. Chim. Acta*, **363**, 3036–3040.
Şen, F., Kansiz, S. & Uçar, İ. (2017). *Acta Cryst.* C**73**, 517–524.
Sheldrick, G. M. (2015*a*). *Acta Cryst.* A**71**, 3–8.

Sheldrick, G. M. (2015*b*). *Acta Cryst.* C**71**, 3–8.
Sliva, T. Yu., Duda, A. M., Głowiak, T., Fritsky, I. O., Amirkhanov, V. M., Mokhir, A. A. & Kozłowski, H. (1997). *J. Chem. Soc. Dalton Trans.* pp. 273–276.
Soujanya, M. & Rajitha, G. (2017). *Int. J. Pharm. Sci. Res*. **8**, 3786–3794.
Spek, A. L. (2009). *Acta Cryst.* D**65**, 148–155.
Stoe & Cie (2002). *X-AREA* and *X-RED32*. Stoe & Cie GmbH, Darmstadt, Germany.
Sudheer, R., Sithambaresan, M., Sajitha, N. R., Manoj, E. & Kurup, M. R. P. (2015). *Acta Cryst.* E**71**, 702–705.
Turner, M. J., MacKinnon, J. J., Wolff, S. K., Grimwood, D. J., Spackman, P. R., Jayatilaka, D. & Spackman, M. A. (2017). *CrystalExplorer17.5*. University of Western Australia, Perth.

supporting information

Acta Cryst. (2018). E**74**, 1628-1632 [https://doi.org/10.1107/S2056989018014627]

Synthesis, crystallographic analysis and Hirshfeld surface analysis of 4-bromo-2-{[2-(5-bromo-2-nitrophenyl)hydrazin-1-ylidene]methyl}-5-fluorophenol

Mavise Yaman, Ercan Aydemir, Necmi Dege, Erbil Agar and Turganbay S. Iskenderov

Computing details

Data collection: *X-AREA* (Stoe & Cie, 2002); cell refinement: *X-AREA* (Stoe & Cie, 2002); data reduction: *X-RED* (Stoe & Cie, 2002); program(s) used to solve structure: SHELXT2014 (Sheldrick, 2015a); program(s) used to refine structure: *SHELXL2017* (Sheldrick, 2015b); molecular graphics: *ORTEP-3 for Windows* (Farrugia, 2012); software used to prepare material for publication: *WinGX* (Farrugia, 2012) and *PLATON* (Spek, 2009).

4-Bromo-2-{[2-(5-bromo-2-nitrophenyl)hydrazin-1-ylidene]methyl}-5-fluorophenol

Crystal data

$C_{13}H_8Br_2FN_3O_3$
$M_r = 433.04$
Monoclinic, $P2_1/n$
$a = 16.1360(14)$ Å
$b = 4.1745(3)$ Å
$c = 21.468(2)$ Å
$\beta = 95.026(7)°$
$V = 1440.5(2)$ Å^3
$Z = 4$
$F(000) = 840$
$D_x = 1.997$ Mg m^{-3}
Mo $K\alpha$ radiation, $\lambda = 0.71073$ Å
Cell parameters from 5914 reflections
$\theta = 1.5$–$29.7°$
$\mu = 5.65$ mm^{-1}
$T = 296$ K
Needle, pink
0.46 × 0.17 × 0.02 mm

Data collection

Stoe IPDS 2 diffractometer
Radiation source: sealed X-ray tube, 12 x 0.4 mm long-fine focus
Detector resolution: 6.67 pixels mm^{-1}
rotation method scans
Absorption correction: integration (X-RED32; Stoe & Cie, 2002)
$T_{min} = 0.296$, $T_{max} = 0.883$
9546 measured reflections
2775 independent reflections
1270 reflections with $I > 2\sigma(I)$
$R_{int} = 0.113$
$\theta_{max} = 26.0°$, $\theta_{min} = 1.5°$
$h = -19\rightarrow19$
$k = -4\rightarrow5$
$l = -26\rightarrow26$

Refinement

Refinement on F^2
Least-squares matrix: full
$R[F^2 > 2\sigma(F^2)] = 0.051$
$wR(F^2) = 0.098$
$S = 0.84$
2775 reflections
200 parameters
0 restraints
Hydrogen site location: inferred from neighbouring sites
H-atom parameters constrained

$w = 1/[\sigma^2(F_o^2) + (0.0267P)^2]$
where $P = (F_o^2 + 2F_c^2)/3$
$(\Delta/\sigma)_{max} < 0.001$

$\Delta\rho_{max} = 0.42$ e Å^{-3}
$\Delta\rho_{min} = -0.28$ e Å^{-3}

Special details

Geometry. All esds (except the esd in the dihedral angle between two l.s. planes) are estimated using the full covariance matrix. The cell esds are taken into account individually in the estimation of esds in distances, angles and torsion angles; correlations between esds in cell parameters are only used when they are defined by crystal symmetry. An approximate (isotropic) treatment of cell esds is used for estimating esds involving l.s. planes.

Fractional atomic coordinates and isotropic or equivalent isotropic displacement parameters (Å²)

	x	*y*	*z*	U_{iso}*/U_{eq}
Br2	0.19136 (4)	−0.4176 (2)	0.67484 (4)	0.0714 (3)
Br1	0.12607 (5)	1.1323 (3)	0.25304 (4)	0.0787 (3)
O3	0.5159 (3)	0.2810 (14)	0.5457 (2)	0.0689 (16)
F1	−0.0194 (2)	0.9500 (15)	0.3236 (2)	0.107 (2)
N1	0.2772 (3)	0.3510 (15)	0.4968 (3)	0.0503 (14)
N3	0.5145 (3)	0.0903 (18)	0.5895 (3)	0.0566 (15)
N2	0.3538 (3)	0.2591 (14)	0.5232 (3)	0.0564 (18)
H2	0.398154	0.325205	0.507843	0.068*
O2	0.5792 (3)	−0.0104 (14)	0.6187 (2)	0.0800 (19)
O1	0.1152 (3)	0.4263 (18)	0.4954 (3)	0.0892 (19)
H1	0.161084	0.357911	0.508414	0.134*
C8	0.3593 (4)	0.0605 (18)	0.5745 (3)	0.0470 (18)
C1	0.1976 (4)	0.8061 (17)	0.3618 (3)	0.0496 (19)
H1A	0.248599	0.848552	0.346371	0.060*
C13	0.4351 (4)	−0.0228 (17)	0.6077 (3)	0.050 (2)
C7	0.2755 (4)	0.5174 (18)	0.4473 (3)	0.050 (2)
H7	0.324917	0.564799	0.430059	0.060*
C11	0.3659 (4)	−0.3285 (19)	0.6826 (3)	0.062 (2)
H11	0.367763	−0.454009	0.718527	0.074*
C12	0.4369 (4)	−0.2110 (18)	0.6608 (3)	0.053 (2)
H12	0.487920	−0.259040	0.682367	0.064*
C6	0.1965 (4)	0.636 (2)	0.4169 (3)	0.0542 (19)
C9	0.2876 (4)	−0.0681 (18)	0.5974 (3)	0.0497 (18)
H9	0.236095	−0.024328	0.576206	0.060*
C10	0.2909 (4)	−0.2535 (18)	0.6492 (3)	0.055 (2)
C2	0.1272 (4)	0.913 (2)	0.3293 (3)	0.0569 (19)
C5	0.1212 (4)	0.584 (2)	0.4414 (3)	0.067 (2)
C4	0.0481 (4)	0.692 (2)	0.4105 (4)	0.078 (3)
H4	−0.002785	0.660131	0.426706	0.093*
C3	0.0533 (4)	0.849 (2)	0.3552 (3)	0.067 (2)

Atomic displacement parameters (Å²)

	U^{11}	U^{22}	U^{33}	U^{12}	U^{13}	U^{23}
Br2	0.0566 (5)	0.0778 (7)	0.0821 (6)	−0.0020 (5)	0.0197 (4)	0.0045 (5)
Br1	0.0781 (6)	0.0915 (8)	0.0632 (5)	−0.0096 (5)	−0.0115 (4)	0.0140 (5)

O3	0.053 (3)	0.084 (5)	0.070 (3)	0.002 (3)	0.007 (3)	0.023 (3)
F1	0.052 (2)	0.167 (6)	0.098 (3)	0.020 (3)	−0.010 (2)	0.037 (3)
N1	0.043 (3)	0.054 (5)	0.053 (4)	0.006 (3)	−0.002 (3)	−0.005 (3)
N3	0.046 (3)	0.066 (5)	0.058 (4)	−0.002 (4)	0.002 (3)	−0.006 (4)
N2	0.040 (3)	0.070 (5)	0.060 (4)	0.003 (3)	0.008 (3)	0.006 (3)
O2	0.040 (3)	0.116 (6)	0.082 (4)	0.010 (3)	−0.006 (3)	0.016 (3)
O1	0.052 (3)	0.136 (6)	0.080 (4)	0.010 (4)	0.011 (3)	0.042 (4)
C8	0.043 (4)	0.056 (5)	0.043 (4)	0.003 (4)	0.005 (3)	−0.004 (4)
C1	0.042 (4)	0.049 (6)	0.058 (5)	−0.001 (3)	0.002 (3)	0.000 (4)
C13	0.040 (4)	0.053 (6)	0.060 (5)	−0.004 (3)	0.007 (3)	−0.006 (4)
C7	0.033 (4)	0.068 (7)	0.048 (4)	−0.004 (3)	0.005 (3)	0.000 (4)
C11	0.064 (5)	0.069 (7)	0.053 (4)	0.007 (4)	0.010 (4)	0.009 (4)
C12	0.043 (4)	0.061 (6)	0.054 (4)	0.009 (4)	−0.004 (3)	−0.003 (4)
C6	0.041 (4)	0.073 (6)	0.047 (4)	−0.002 (4)	0.001 (3)	0.001 (4)
C9	0.041 (4)	0.047 (5)	0.061 (4)	0.007 (4)	0.007 (3)	−0.011 (4)
C10	0.059 (4)	0.056 (6)	0.049 (4)	0.012 (4)	0.006 (4)	−0.001 (4)
C2	0.049 (4)	0.059 (5)	0.062 (4)	−0.003 (4)	0.003 (3)	−0.007 (4)
C5	0.041 (4)	0.097 (7)	0.064 (5)	0.003 (5)	0.010 (4)	0.018 (5)
C4	0.042 (4)	0.124 (9)	0.069 (5)	0.008 (5)	0.012 (4)	0.015 (5)
C3	0.041 (4)	0.093 (7)	0.062 (5)	0.009 (4)	−0.019 (4)	−0.002 (5)

Geometric parameters (Å, º)

Br2—C10	1.872 (7)	C1—H1A	0.9300
Br1—C2	1.874 (7)	C13—C12	1.383 (9)
O3—N3	1.234 (7)	C7—C6	1.465 (9)
F1—C3	1.369 (7)	C7—H7	0.9300
N1—C7	1.268 (8)	C11—C12	1.366 (9)
N1—N2	1.368 (7)	C11—C10	1.388 (9)
N3—O2	1.243 (7)	C11—H11	0.9300
N3—C13	1.451 (8)	C12—H12	0.9300
N2—C8	1.374 (8)	C6—C5	1.383 (8)
N2—H2	0.8600	C9—C10	1.353 (10)
O1—C5	1.343 (8)	C9—H9	0.9300
O1—H1	0.8200	C2—C3	1.386 (9)
C8—C9	1.402 (8)	C5—C4	1.378 (10)
C8—C13	1.406 (9)	C4—C3	1.363 (10)
C1—C2	1.356 (9)	C4—H4	0.9300
C1—C6	1.381 (9)		
C7—N1—N2	117.0 (5)	C11—C12—H12	119.0
O3—N3—O2	122.2 (6)	C13—C12—H12	119.0
O3—N3—C13	119.4 (6)	C1—C6—C5	119.0 (6)
O2—N3—C13	118.4 (6)	C1—C6—C7	118.6 (6)
N1—N2—C8	119.6 (5)	C5—C6—C7	122.4 (6)
N1—N2—H2	120.2	C10—C9—C8	122.3 (6)
C8—N2—H2	120.2	C10—C9—H9	118.9
C5—O1—H1	109.5	C8—C9—H9	118.9

N2—C8—C9	120.9 (6)	C9—C10—C11	121.6 (7)
N2—C8—C13	123.3 (6)	C9—C10—Br2	118.6 (5)
C9—C8—C13	115.8 (6)	C11—C10—Br2	119.8 (6)
C2—C1—C6	122.5 (6)	C1—C2—C3	116.2 (7)
C2—C1—H1A	118.8	C1—C2—Br1	123.6 (5)
C6—C1—H1A	118.8	C3—C2—Br1	120.1 (5)
C12—C13—C8	120.9 (6)	O1—C5—C4	116.9 (6)
C12—C13—N3	116.9 (6)	O1—C5—C6	122.5 (6)
C8—C13—N3	122.2 (6)	C4—C5—C6	120.5 (7)
N1—C7—C6	120.9 (6)	C3—C4—C5	117.5 (6)
N1—C7—H7	119.6	C3—C4—H4	121.2
C6—C7—H7	119.6	C5—C4—H4	121.2
C12—C11—C10	117.5 (7)	C4—C3—F1	117.7 (6)
C12—C11—H11	121.2	C4—C3—C2	124.2 (6)
C10—C11—H11	121.2	F1—C3—C2	118.1 (7)
C11—C12—C13	122.0 (6)		

C7—N1—N2—C8	−175.6 (6)	C13—C8—C9—C10	1.7 (10)
N1—N2—C8—C9	4.6 (10)	C8—C9—C10—C11	−0.3 (12)
N1—N2—C8—C13	−174.2 (6)	C8—C9—C10—Br2	−179.0 (5)
N2—C8—C13—C12	176.8 (7)	C12—C11—C10—C9	−0.7 (11)
C9—C8—C13—C12	−2.1 (10)	C12—C11—C10—Br2	178.0 (5)
N2—C8—C13—N3	−1.4 (10)	C6—C1—C2—C3	1.4 (12)
C9—C8—C13—N3	179.7 (6)	C6—C1—C2—Br1	−177.9 (6)
O3—N3—C13—C12	−173.8 (7)	C1—C6—C5—O1	−178.7 (8)
O2—N3—C13—C12	6.4 (9)	C7—C6—C5—O1	1.5 (13)
O3—N3—C13—C8	4.4 (10)	C1—C6—C5—C4	1.6 (13)
O2—N3—C13—C8	−175.3 (7)	C7—C6—C5—C4	−178.3 (8)
N2—N1—C7—C6	−177.9 (6)	O1—C5—C4—C3	−179.2 (9)
C10—C11—C12—C13	0.3 (11)	C6—C5—C4—C3	0.6 (14)
C8—C13—C12—C11	1.2 (11)	C5—C4—C3—F1	178.3 (8)
N3—C13—C12—C11	179.5 (7)	C5—C4—C3—C2	−1.9 (14)
C2—C1—C6—C5	−2.6 (12)	C1—C2—C3—C4	1.0 (13)
C2—C1—C6—C7	177.3 (7)	Br1—C2—C3—C4	−179.8 (8)
N1—C7—C6—C1	−177.6 (7)	C1—C2—C3—F1	−179.3 (7)
N1—C7—C6—C5	2.3 (12)	Br1—C2—C3—F1	−0.1 (11)
N2—C8—C9—C10	−177.2 (7)		

Hydrogen-bond geometry (Å, º)

D—H···*A*	*D*—H	H···*A*	*D*···*A*	*D*—H···*A*
O1—H1···N1	0.82	1.91	2.631 (7)	146
N2—H2···O3	0.86	2.01	2.619 (7)	127
N2—H2···O3^{i}	0.86	2.50	3.293 (7)	155
C4—H4···O1^{ii}	0.93	2.60	3.494 (8)	162

C7—H7···O3^{i}	0.93	2.66	3.461 (7)	145
C12—H12···Br1^{iii}	0.93	3.02	3.908 (7)	161

Symmetry codes: (i) −*x*+1, −*y*+1, −*z*+1; (ii) −*x*, −*y*+1, −*z*+1; (iii) *x*+1/2, −*y*+1/2, *z*+1/2.